Title
LEED, AES AND THERMAL DESORPTION STUDIES OF THE OXIDATION OF THE RHODIUM (111) SURFACE

Author
Castner, D.G.

Publication Date
1979-06-01

Lawrence Berkeley Laboratory

UNIVERSITY OF CALIFORNIA, BERKELEY, CA

Materials & Molecular Research Division

Submitted to Applications of Surface Science

LEED, AES AND THERMAL DESORPTION STUDIES OF THE OXIDATION OF THE RHODIUM (111) SURFACE

D. G. Castner and G. A. Somorjai

June 1979

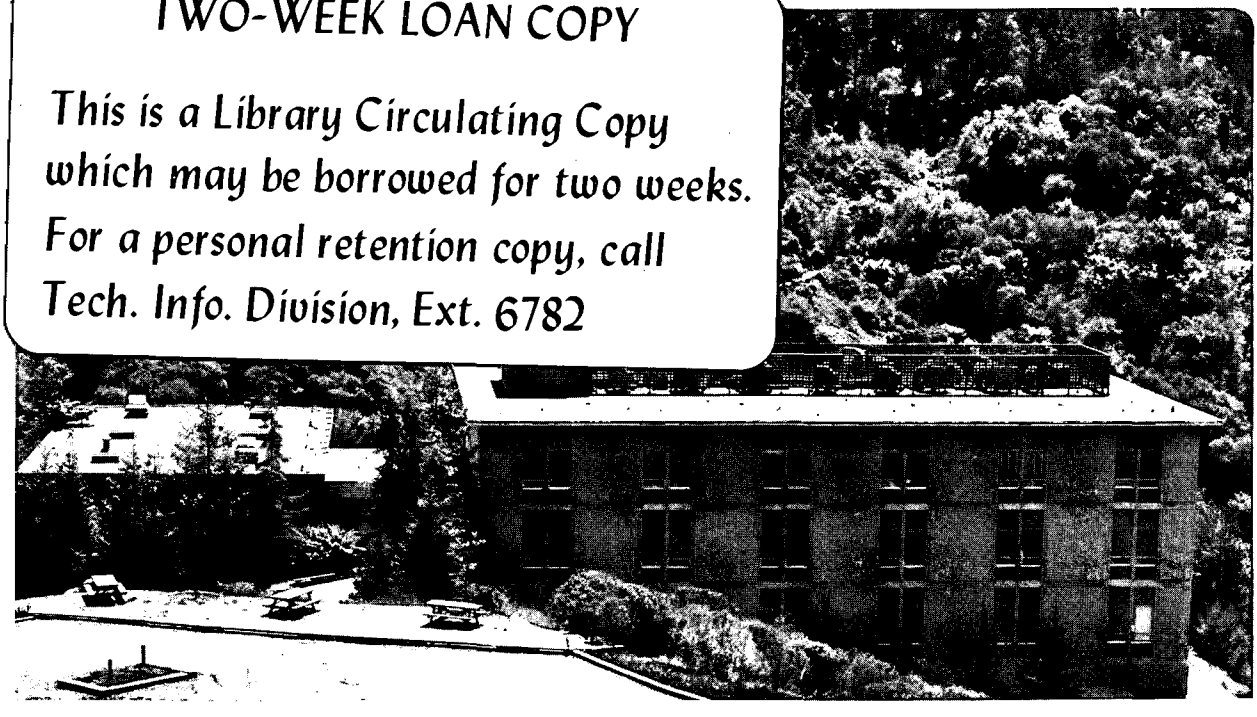

Prepared for the U. S. Department of Energy
under Contract W-7405-ENG-48

DISCLAIMER

LBL 9288

Submitted to Applications of Surface Science

LEED, AES AND THERMAL DESORPTION STUDIES OF THE OXIDATION OF THE RHODIUM (111) SURFACE

D.G. Castner*and G.A. Somorjai

Department of Chemistry, University of California

Materials and Molecular Research Division
Lawrence Berkeley Laboratory
Berkeley, CA 94720

*Present Address: Chevron Research Company, P.O. Box 1627, Richmond, CA 94802

Abstract

The oxidation of the Rh(111) surface was studied by low-energy electron diffraction (LEED), Auger electron spectroscopy (AES) and thermal desorption mass spectroscopy (TDS). Four different oxygen species were detected during the oxidation. Initially chemisorbed oxygen atoms are produced from the low temperature dissociative adsorption of oxygen and undergo an activated ordering process to form three domains of a (2x1) structure. The chemisorbed oxygen was readily removed by exposure to hydrogen above 350 K. Heating the Rh(111) crystal in the presence of oxygen resulted in oxygen diffusing into the near surface region. Prolonged high temperature annealing produced an unreactive surface oxide. The epitaxial growth of Rh_2O_3(0001) on Rh(111) occurred during high temperature annealing in 1 torr of O_2. This epitaxial oxide did not adsorb detectable amounts of either hydrogen or CO at 300 K and could be decomposed by heating the crystal to 800 K in vacuum.

1. Introduction

In this paper we report the results of oxidation studies on Rh(111) from the initial oxygen chemisorption stage through the growth of epitaxial Rh oxide. Past oxidation studies on single crystal Rh surfaces have primarily investigated oxygen chemisorption.[1-9] Oxidation studies of the other Group VIII transition metals have been carried out by a variety of surface sensitive techniques and ordered oxygen structures have been observed on the single crystal surfaces of all of these metals except osmium.[10] In particular the hexagonal faces of Ir,[11,12] Ni,[13] Pd,[14] Pt,[15] Rh [1,3,5] and Ru [5,16] all form apparent (2x2) surface structures during oxygen chemisorption. Oxygen (2x2) structures with coverages of θ=1/4 have been proposed for Ni[13] and Pd[14] while three domains of a (2x1) structure with θ=1/2 have been suggested for Ir[11,12], Pt[15] and Ru.[16] Previous studies of oxygen chemisorption on Rh(111) [1,3,5] have not been able to differentiate between the two structural possibilities. The results of our investigation indicate that the ordered chemisorbed oxygen structure on Rh(111) is three domains of a (2x1) structure. Ordered epitaxial oxides have been observed on the hexagonal faces of Co[17], Ir[18], Ni[19], Pd[14] and Pt[20] but not on Rh or Ru. In this paper we report the epitaxial growth of Rh_2O_3(0001) on the Rh(111) surface. Low-energy electron diffraction (LEED) was used to detect the formation of surface structures. Auger electron spectroscopy (AES) was used to monitor the surface composition. Thermal desorption mass spectroscopy (TDS) was used to obtain information about the binding and desorption of the oxygen species and their diffusion into the near surface region.

In this investigation we were able to identify four different types of oxygen species: chemisorbed oxygen atoms, dissolved oxygen in the rhodium

lattice, a "strongly bound oxygen" and epitaxial Rh_2O_3. The chemisorption results reported in this paper are in good agreement with and add new information to previous studies of oxygen chemisorption on Rh(111).[1,3,5] We also report the first observation of ordered epitaxial oxide formation on Rh(111). Our results will be compared with the previous results of oxidation studies on other Group VIII transition metal single crystal surfaces.

2. Experimental

The experiments were carried out in a Varian ion pumped UHV system having LEED, retarding field AES and TDS capabilities. The Rh(111) crystal was a 1 mm thick, 6 mm diameter disc oriented within $\pm 1/2°$ of the (111) crystal face. The crystal was mechanically polished with the final polishing done on a syntron containing a slurry of 0.05μ Al_2O_3 in H_2O.

The crystal was connected to 1/4 inch square Cu bar supports by 0.007 inch thick Ta foil, with the rhodium crystal attached to the Ta foil by spot welds. The sample was mounted such that the Ta foil masked off the back side of the crystal. The heating leads outside the vacuum chamber were LN_2 cooled so adsorptions could be carried out at temperatures between 210 and 1075 K. The crystals were heated resistively and the crystal temperature was monitored by a chromel-alumel thermocouple spot welded to the back side of the crystal. Sulfur, boron and carbon were the major impurities detected on the Rh(111) surface and were removed by argon ion bombardment and annealing. Boron, which is a major bulk impurity (17 ppm), segregated to the surface and required many cycles of ion bombardment (500 eV, 5×10^{-5} torr Ar,300K) and annealing at 1070 K to deplete it from the near surface region.

Oxygen adsorption was studied for O_2 pressures between $1x10^{-8}$ torr and 1 torr and at temperatures between 210 and 1075 K. Surface structures were observed both with increasing exposure and after the gas was pumped away. Oxygen TDS spectra were taken by plotting the output of mass number 32 from the quadrupole mass spectrometer (UTI model 100C) versus temperature while the crystal temperature was being increased linearly. Blank TDS experiments were performed by replacing the Rh crystal with Ta foil to insure that desorption peaks in the rhodium TDS spectra were from the Rh(111) crystal and not the Ta foil supports.

The conditions (O_2 partial pressure, crystal temperature, time) for formation of the various oxygen species described in Section 3 did not always generate reproducible amounts of the various oxygen species. This was particularly true for the formation of the strongly bound oxygen and epitaxial oxide.. For these cases additional variables such as the pressure of the residual background gases, the presence of impurities in the surface and/or near surface region and the previous oxygen and heat treatments of the sample were found to be important. The conditions given in Section 3 are for oxygen exposures on a clean surface (as determined by AES) in a well baked UHV system with all filaments and the crystal holder thoroughly degased to keep the pressures of the residual background gases at a minimum. The pressures were measured by a nude ionization gauge and were not corrected for the sensitivity differences of the ionization gauge to the various gases.

3. Results

a. LEED Results of the Oxidation Study on the Rh(111) Surface.

The adsorption of 10 L (1 L = $1x10^{-6}$ torr·sec) of oxygen at 210K on the

clean Rh(111) surface resulted in the appearance of large diffuse diffraction beams at the half order positions. These new diffraction features were slightly elongated and by rapidly cooling the clean Rh(111) surface from 500 to 210K (~50 sec) in an oxygen pressure of 2×10^{-7} torr they became sharper and the elongation more pronounced. The diffraction pattern observed during this rapid cooling in oxygen is shown in Fig.1b. The diffraction pattern in Fig.1c with sharp half order diffraction spots was obtained by either flashing the pattern in Fig.1b to 300 K in an oxygen pressure of 1×10^{-7} torr or adsorbing 10 L of oxygen on a clean Rh(111) surface at 300 K. If the crystal was cooled to 210 K after formation of the sharp half order diffraction spots, the spots remained sharp. These results indicate the ordering of the chemisorbed oxygen overlayer on Rh(111) is an activated process.

Two different surface structures, a (2x2) or three domains of a (2x1), can generate a LEED pattern with sharp half order diffraction spots (Fig.1c). In Fig.2 the unit cells of the (2x2) structure and one domain of the c(2x2) and (2x1) structures are shown. Both the c(2x2) and (2x1) unit cells describe identical oxygen overlayers; therefore, for the remainder of this paper we will primarily refer to it as a (2x1) structure. We have used the activated ordering process to differentiate between the (2x1) and (2x2) structures on Rh(111). By following the shape of the half order diffraction features during the ordering process, it was determined that three domains of (2x1) structure was consistent with the direction of spot elongation (Fig.1b). This is illustrated in Fig.3. Fig. 3a shows the schematic LEED pattern of Fig.1b and the reciprocal space unit cells of the (2x1) and c(2x2) structures. Only one direction of elongation or streaking of the diffraction features is present in the (2x1) and c(2x2) unit cells and this

streaking corresponds to disorder along the rows of oxygen atoms in the (2x1) structure. As shown schematically in Fig.3b, the (2x2) reciprocal space unit cell only indexes a half order diffraction pattern with sharp spots. If the (2x2) reciprocal space unit cell was used to index the schematic LEED pattern in Fig.3a, it would contain three different directions of elongated diffraction features, corresponding to disorder in three crystallographic directions. Disordering in three directions of the (2x2) structure would tend to make the half order diffraction features round, broad and diffuse, not elongated as shown in Fig.3a. Therefore chemisorbed oxygen forms a (2x1)-O surface structure on Rh(111). The chemisorbed oxygen species present in the (2x1) structures was very reactive with hydrogen and the half order diffraction features shown in Figs. 1b and 1c were rapidly removed when the rhodium surface was heated to 350K in $1x10^{-7}$ torr of H_2.

Further oxidation of the rhodium surface was carried out by heating the crystal to high temperatures in the presence of oxygen. For temperatures up to 1075 K and oxygen pressures up to $1x10^{-5}$ torr only half order diffraction spots were observed in the LEED pattern. Although this is the same diffraction pattern as was seen for chemisorbed oxygen, the reativity with hydrogen of the oxygen species that make up this surface structure was much lower than was observed for the chemisorbed oxygen. After prolonged heating (>30 min.) at 1075 K in $1x10^{-5}$ torr of O_2, the half order diffraction spots could not be removed by heating the crystal to 350 K in $1x10^{-7}$ torr of H_2 and high temperature anneals (1175 K) in hydrogen were required to regenerate the clean Rh(111) surface. This unreactive oxygen species has also been referred to as "strongly bound oxygen" or "surface oxide" in the literature and we use these three descriptions interchangeably here.

Increasing the oxygen pressure to 1 torr and heating the crystal at 975K for 10 minutes resulted in the appearance of a diffraction pattern from a (8x8) surface structure (Fig.1d). This (8x8) coincidence lattice structure can be identified as the epitaxial growth of $Rh_2O_3(0001)$ on the Rh(111) surface. Rh_2O_3 has the corundum structure with unit cell vectors of a=5.108Å and c=13.81Å.[21] Four unit cells of $Rh_2O_3(0001)$, expanded by 5%, would fit into an (8x8) structure on Rh(111). The formation of a slightly expanded hexagonal Rh_2O_3 structure at 975K in 1 torr of O_2 is reasonable since the corundum form of Rh_2O_3 expands into an orthorhombic structure with unit cell vectors of a=5.149Å and c=14.688Å when heated above 1025K in air.[21] The corundum structure is just a hexagonal closest packed (hcp) lattice of oxide ions with 2/3 of the octahedral holes occupied by metal ions. The basal plane of Rh_2O_3 would consist of an hcp layer of oxide ions with Rh ions arranged in the threefold hollow sites of the oxygen layer to form a $(\sqrt{3}x\sqrt{3})R30°$ structure (see Fig.4).

Epitaxial Rh_2O_3 was inert and neither hydrogen nor CO adsorption could be detected on this surface at 300K. The (8x8) structure could be removed by either heating the crystal to 800K in vacuum or to 1075K in $1x10^{-5}$ torr of O_2. Rh_2O_3 decomposes in air at 1325;[21] thus the oxide decomposition temperature increases as the partial pressure of O_2 above the oxide is increased.

b. AES Results of the Oxidation Study on the Rh(111) Surface.

The AES spectra for the Rh(111)-oxygen system are shown in Figs.5 and 6. The spectra in Fig.5 show the rhodium MNN and oxygen KLL transitions. In Fig.6 the rhodium NVV transition is shown. The low energy NVV transition involves the d band electrons and, therefore, is ideally suited for following the changes which occur in the d band during oxidation. The top spectra in Figs. 5 and 6 are for the clean Rh(111) surface. Adsorbing 10 L of oxygen at 300K on a clean Rh(111) surface

results in the appearance of low intensity oxygen transitions at 496 and 518 eV (middle spectrum of Fig.5). The O_{518}/Rh_{302} peak-to-peak ratio in this spectrum is 0.06. No change in the 39 eV rhodium transition was detected during oxygen adsorption at 300 K. High temperature oxidation of the rhodium surface resulted in the oxygen transitions growing in intensity and shifting to lower energies. The bottom spectrum in Fig.5 is from a Rh(111) crystal with an epitaxial layer of $Rh_2O_3(0001)$. In this spectrum the major oxygen transition has shifted from 518 eV to 515 eV and has a O_{515}/Rh_{302} peak-to-peak ratio of 0.25. High temperature oxidation also resulted in the appearance of a transition from Rh oxide at 35 eV. This transition grew in intensity as the amount of oxygen in the near-surface region increased. The spectra in Figs. 6a and 6b are from surfaces with O_{515}/Rh_{302} peak-to-peak ratios of 0.18 and 0.25, respectively. Due to the small energy difference between the 35 and 39 eV peaks and the modulation voltage used (2 eV, peak-to-peak) these peaks were not well resolved. The 35 eV Rh oxide transition was also broader than the 39 eV transition of the clean Rh(111) surface. These results indicate the Rh oxide d band is broader and shifted downward in energy relative to the metallic Rh d band.

c. TDS Results of the Oxidation Study on the Rh(111) Surface.

The TDS spectra for oxygen adsorbed at 300 K on a clean Rh(111) surface are shown in Fig.7. For low O_2 exposures no oxygen desorption (mass 32) was detected. An oxygen signal was present in the AES spectrum before but not after the desorption experiments. This adsorbed oxygen was not being removed during the desorption experiments by any near surface region impurities or residual background gases since no desorption of any oxygen containing species (CO, CO_2, H_2O, etc.) was detected. The lack of oxygen desorption can be explained

by diffusion of oxygen into the near surface region. The diffusion of oxygen into the near surface region has been previously observed on rhodium.[1-3,9] After higher O_2 exposures oxygen desorbed from the rhodium surface and the desorption temperature decreased with increasing O_2 exposure. The TDS spectrum of chemisorbed oxygen is characteristic of a second order desorption process, indicating that two oxygen atoms recombine at a slow rate to form an oxygen molecule before desorbing. This implies that O_2 is dissociatively adsorbed since this would provide the source of oxygen atoms needed for a second order desorption process.

Hydrogen, oxygen and CO TDS experiments were attempted on the oxidized (8x8) surface structure so that a comparison with TDS results on clean rhodium surfaces could be made. It was found that neither hydrogen nor CO adsorbed in sufficient amounts to be detectible on the (8x8) structure at 300 K. and the (8x8) structure began decomposing as the crystal was heated during the desorption experiments. For this reason only the decomposition of the epitaxial oxide was investigated. Heating the oxidized surface to 800 K resulted in a large oxygen (mass 32) desorption signal as the epitaxial oxide LEED pattern reverted to a half order LEED pattern. If this pattern was then heated to 1200 K a large oxygen desorption signal (more than 100 times the signal from the chemisorbed oxygen in Fig.7) was observed between 800 and 1200 K. The initial heating to 800 K decomposed the epitaxial Rh_2O_3, but still left a large amount of oxygen in the near surface region which could be removed by heating the crystal to 1200 K. Most of the oxygen removed at this temperature must be from the near surface region, since the amount of oxygen desorbed was far too large to be just due to a monolayer of adsorbed oxygen. The size of this desorption peak indicates

that the rhodium lattice can dissolve large amounts of oxygen. Thus, oxidation of the Rh(111) surface not only results in the epitaxial growth of $Rh_2O_3(0001)$ but also the dissolution of oxygen into the near surface region

4. Discussion

Four different oxygen species can be identified during the oxidation of the Rh(111) surface: chemisorbed oxygen atoms, oxygen dissolved in the rhodium lattice, surface oxide and epitaxial $Rh_2O_3(0001)$. The production of these four oxygen species is interdependent and interconversion between the different species could be accomplished by making the appropriate changes in O_2 partial pressure and crystal temperature. This section will contain a general discussion of the oxidation properties of the Rh(111) surface and a comparison of these properties to other Rh crystal faces and other transition metals.

The chemical and structural properties of the chemisorbed oxygen species on Rh(111) has been extensively discussed and compared to other Group VIII transition metals in previous investigations.[1,3-5] Our present results are in good agreement with the previous work. Chemisorbed oxygen atoms were produced by low temperature dissociative adsorption of oxygen. Dissociative adsorption of O_2 and the resulting second order desorption kinetics indicated by our results are consistent with previous investigations on Rh(111),[1-3] Ir(111)[11,12] and Pd(111)[14]. More evidence for O_2 dissociative adsorption can be obtained from high resolution electron loss spectroscopy (ELS) experiments. Oxygen adsorption on Rh(111) produces a single loss peak at 520 cm^{-1} in the ELS spectrum.[22] This peak is the metal-oxygen stretch of a chemisorbed oxygen atom and falls in the range of values seen for the metal-oxygen stretching frequencies on Cu[23], Ni[24], Ru[25] and W[26].

Chemisorbed oxygen produces half order diffraction patterns on the hexagonal surfaces of Ir[11,12], Ni[13], Pd[14], Pt[15], Rh[1,3,5] and Ru[5,16]. Several methods have been used to determine whether these half order diffraction patterns are from a (2x2) or three domains of a (2x1) surface structure. LEED surface crystallography investigations of the Ni(111)-oxygen[27] and Ir(111)-oxygen[28] systems have been undertaken. These studies were unable to differentiate between the two structures but did determine that the oxygen atoms resided in threefold hollow sites. On Ir (111)[11] the activated ordering of oxygen was used to determine that chemisorbed oxygen forms a (2x1) surface structure, just as in our studies on Rh(111). A previous low temperature study of oxygen adsorption on Rh(111)[3] found that ordering of the oxygen overlayer was activated, but did not identify whether the oxygen structure was a (2x1) or (2x2) structure. Determination of surface coverage has also been used to make the distinction between the (2x1) and (2x2) structures since for the (2x1) structure θ=1/2 while for the (2x2) structure θ could be 1/4, 1/2 or 3/4 (in Fig. 2, θ=1/4 is shown). On Ni(111)[13] and Pd(111)[14] $(\sqrt{3}x\sqrt{3})R30°$-O structures with θ=1/3 are observed at oxygen coverages higher than those in the (2x2)-O structures, implying that a true (2x2) surface structure with θ=1/4 is formed on Ni and Pd. On Ir(111), Pt(111), Rh(111) and Ru(0001) a $(\sqrt{3}x\sqrt{3})30°$ structure has not been observed for chemisorbed oxygen. For Ir(111)[11,12], Pt(111)[15] and Ru(0001)[16] surface coverage measurements have shown θ=1/2 and three domains of a (2x1) structure have been suggested to be the proper structure.

Heating the crystal in the presence of oxygen results in the dissolution of oxygen into the rhodium lattice. If the oxygen pressure and crystal temperature are high enough, oxide formation will occur in addition to the dissolution of oxygen. At the highest oxygen pressures and crystal temperatures,

the growth of epitaxial Rh_2O_3 is observed. Thus, while initially low temperature oxygen adsorption just produces chemisorbed oxygen once the temperature is raised, oxygen interaction with the Rh(111) surface rapidly becomes much more complex. The two extreme stages of Rh(111) oxidation, the initial chemisorbed oxygen and the final epitaxial oxide, are the easiest to characterize, but the intermediate stages where the nonreactive surface oxide and dissolved oxygen are present are probably of more catalytic importance. Rh_2O_3 would only be stable under highly oxidizing conditions, while chemisorbed oxygen would rapidly be converted to H_2O or CO_2 if any H_2 or CO were present. The non-reactive surface oxide and dissolved oxygen, however, would be much more stable under reaction conditions and could alter the catalytic properties of rhodium. For CO hydrogenation over polycrystalline Rh[29] and Rh(111)[30] catalysts oxygen pretreatment resulted in both an increase in activity and a change in selectivity. On Pt single crystal catalysts the formation of a surface oxide increased dehydrogenation and hydrogenation activities and changed the dehydrogenation-hydrogenation selectivity.[31] The oxygen AES signal from the surface oxide on Rh[30] and Pt[31] remained constant throughout the experiments indicating these surface oxides were not removed under the reaction conditions. Nonreactive oxygen species have also been formed by high temperature oxidation of the Ir(111)[12] and Pd(111)[14] surfaces.

The structure sensitivity of the platinum metal surface oxides should also be considered. On Pt surfaces preoxidation yielded a higher relative enhancement of dehydrogenation and hydrogenation activities for a kinked surface than for a stepped or flat surface.[31] Oxygen diffusion into the near surface region of Pd was found to be more pronounced on the (111) than on the (110) surface.[14] For Rh oxygen dissolution and nonreactive surface oxide formation

has been observed on the (111)[1,3], (100)[1,7], (110)[6,9] and several stepped[2,8] surfaces.

The relationship of dissolved oxygen to these surface oxides is also important to consider. One possibility that our results suggest is that only after the near surface region becomes saturated with dissolved oxygen does oxygen precipitate at the surface and form the surface oxide. This is reasonable since at the high temperatures needed to form the surface oxide oxygen is soluble in the rhodium lattice and the crystal must be heated for extended periods of time to form the nonreactive surface oxide. If this is the case, then dissolved oxygen and the surface oxide are very closely related and it will be important to consider the oxygen concentration gradient in the near surface region. Large changes in the oxygen concentration profile could occur that would not be detected by AES if the oxygen concentration in the upper two or three layers was not markedly affected. The low energy AES transitions are useful in following changes in the distribution of valence band electrons during oxidation, but use of the oxygen AES signal to follow changes in the oxygen concentrations during reactions may be misleading.

Epitaxial growth of Rh_2O_3 has not previously been reported on rhodium single crystals but studies on Rh(110)[6,9] observed the formation of several ordered surface structures when the crystal was heated in oxygen. Some of these structures were proposed to contain an adlayer of rhodium and oxygen atoms.[6] The growth of epitaxial oxides has been observed on most of the other Group VIII transition metals, however. In Table I the surface orientation and approximate temperatures of formation of these epitaxially grown transition metal oxides have been summarized.

The transition metals in Table I can be divided into two groups, the

3d metals (Fe, Co, Ni) which readily form epitaxial oxides at or near room temperature and the platinum metals (Rh, Pd, Ir, Pt) which are much more resistant to oxidation and only exhibit epitaxial oxide formation at high temperatures. This difference generates distinctly different behavior of these two groups during oxidation. For the 3d metals oxidation proceeds directly from chemisorbed oxygen to the epitaxial oxide.[17,19,32] On the platinum metals, there are large temperature differences between the chemisorbed oxygen and the epitaxial oxide growth stages and dissolved oxygen and nonreactive surface oxides are formed during the intermediate stages of oxidation.[12,14,31]

Our AES results on oxidized Rh(111) are in good agreement with results on other oxidized transition metals. On Pt[20,34] and Ni[35] the oxygen KLL transitions shift to lower energies during oxidation by 6 and 1.7 eV, respectively, similar to the 3 eV shift we encountered for the Rh-oxygen system. The oxidation of Zn produced low energy AES transitions from Zn oxide which were broader and shifted downward in energy by 3 to 4 eV compared to the low energy AES transitions of clean Zn,[36] as is the case for oxidized Rh. For Zn[36] the broadening and shift of the low energy oxide peaks have been interpreted as an increase in the d band width and variation of extra-atomic relaxation energies. Peak broadening and shifts have also been seen on oxidized Ni[35,37,38], resulting from differences between the d band in Ni oxide and metallic Ni. A low energy oxide peak shifted downward 3 eV in energy from the low energy metallic peak has been observed during the oxidation of Fe(001)[32] and was interpreted as resulting from positively charged Fe in an Fe oxide phase.

5. Conclusions

In our investigation of the oxidation of the Rh(111) surface, we have identified and characterized the following four oxygen species:

1. Low temperature dissociative adsorption produced very reactive chemisorbed oxygen atoms which underwent an activated ordering process to form three domains of a (2x1) surface structure.

2. Heating the crystal in the presence of oxygen resulted in dissolution of large amounts of oxygen in the rhodium lattice.

3. Prolonged high temperature annealing in 1×10^{-5} torr of O_2 produced a nonreative surface oxide.

4. High temperature annealing in 1 torr of O_2 resulted in an epitaxial growth of $Rh_2O_3(0001)$ on the Rh(111) surface.

6. Acknowledgement

Several very informative conversations with L.H. Dubois are gratefully acknowledged.

This work was supported by the Division of Materials Sciences, Office of Basic Energy Sciences, U.S. Department of Energy.

D.G. C[illegible] acknowledges an N.S.F. Energy Fellowship.

7. References

1. D.G. Castner, B.A. Sexton and G.A. Somorjai, Surface Sci. 71,519 (1978).
2. D.G. Castner and G.A. Somorjai, Surface Sci. 83,60 (1979).
3. P.A. Thiel, J.T. Yates and W.H. Weinberg, Surface Sci. 82,22 (1979).
4. J.T. Yates, P.A. Thiel and W.H. Weinberg, Surface Sci. 82, 45 (1979).
5. J.T. Grant and T.W. Haas, Surface Sci. 21, 76 (1970).
6. C.W. Tucker, J. Appl. Phys. 37, 4147 (1966) and 38, 2696 (1967).
7. C.W. Tucker, Acta Metallurgica 15, 1465 (1967).
8. C.W. Tucker, J. Appl. Phys. 37, 3013 (1966).
9. R.A. Marbrow, Ph.D. Thesis, University of Cambridge, 1977.
10. D.G. Castner and G.A. Somorjai, Chemical Reviews 79, 233 (1979).
11. D.I. Hagen, B.E. Nieuwenhuys, G.Rovida and G.A. Somorjai, Surface Sci. 57,632 (1976).
12. V.P. Ivanov, G.K. Boreskov, V.I. Savchenko, W.F.Egelhoff and W.H. Weinberg Surface Sci. 61, 207 (1976).
13. H. Conrad, G. Ertl, J. Küppers and E.E. Latta, Surface Sci. 57, 475 (1976).
14. H. Conrad, G. Ertl, J. Küppers and E.E. Latta, Surface Sci. 65, 245 (1977).
15. H.P. Bonzel and R. Ku, Surface Sci. 40, 85 (1973).
16. T.E. Madey, H.A. Engelhardt and D. Menzel, Surface Sci. 48, 304 (1975).
17. M.E. Bridge and R.M. Lambert, Surface Sci. 82, 413 (1979).
18. H. Conrad, J. Küppers, F. Nitschké and A. Plagge, Surface Sci. 69, 668 (1977).
19. H. Conrad, G. Ertl, J. Küppers and E.E. Latta, Solid State Comm. 17, 497 (1975).
20. P. Légaré, G. Maire, B. Carière and J.P. Deville, Surface Sci. 68, 348 (1977).
21. A. Wold, R.J. Arnott and W.J. Croft, Inorganic Chemistry 2, 972 (1963).
22. L.H. Dubois and G.A. Somorjai, LBL 9280.
23. B.A. Sexton, to be published.
24. S. Andersson, Solid State Comm. 20, 229 (1976).
25. G.E. Thomas and W.H. Weinberg, J. Chem. Phys. 70, 954 (1979).
26. H. Froitzheim, H. Ibach and S. Lehwald, Phys. Rev. B14, 1362 (1976).
27. P.M. Marcus, J.E. Demuth and D.W. Jepsen, Surface Sci. 53, 501 (1975).
28. C.M. Chen and W.H. Weingerg, to be published.
29. B.A. Sexton and G.A. Somorjai, J.Catal. 46, 167 (1977).
30. D.G. Castner, R.L. Blackadar and G.A. Somorjai, to be published.

31. C.E. Smith, J.P. Biberian and G.A. Somorjai, J. Catal. 57, 426 (1979).
32. G.W. Simmons and D.J. Dwyer, Surface Sci. 48, 373 (1975).
33. R. Ducros and R.P. Merrill, Surface Sci. 55, 227 (1976).
34. T. Matsushima, D.B. Almy and J.M. White, Surface Sci. 67, 89 (1977).
35. C. Benndorf, B. Egert, G. Keller, H.Seidel and F. Thieme, Surface Sci. 80. 287 (1979).
36. S. Ferrer, A.M. Baró and J.M. Rojo, Surface Sci. 64, 668 (1977).
37. P.H. Holloway and J.B. Hudson, J. Vac. Sci. Technol. 12, 647 (1975).
38. A.M. Horgan and I.Dalins, Surface Sci. 36, 526 (1973).

Table I

The Structure and Approximate Temperatures of Epitaxial Oxide Formation on the Group VIII Transition Metals

Substrate	Epitaxial Oxide	Approximate Temperatures of Epitaxial Oxide Formation (K)	Reference
Fe(001)	FeO(001)	575	32
Fe(001)	FeO(111)	575	32
Co(0001)	CoO(111)	300	17
Co(0001)	Co_3O_4(111)	600	17
Ni(111)	NiO(111)	300	19
Rh(111)	Rh_2O_3(0001)	975	this study
Pd(111)	PdO(100)	1000	14
Ir(111)	Ir oxide	1300	18
Pt(111)	PtO_2(0001)	1275	20
Pt(110)	PtO(100)	1075	33

8. Figure Captions

Fig.1 Oxygen LEED patterns on Rh(111). (a) the clean Rh(111) surface at 64.5 eV; (b) slightly disordered Rh(111)-(2x1)-O at 67 eV; (c) well ordered Rh(111)-(2x1)-O at 67 eV; (d) Rh(111)-(8x8) coincidence lattice from $Rh_2O_3(0001)||Rh(111)$ at 73 eV.

Fig.2 Real space unit cells for (2x2), c(2x2) and (2x1) surface structures on Rh(111). The large circles represent the rhodium atoms and the small circles represent the oxygen atoms. The (1x1) structure is the unit cell of the Rh(111) surface. The rhodium nearest neighbor distance is 2.69Å. The oxygen atoms have arbitrarily been placed in the three-fold hollow sites and only one domain of the c(2x2) and (2x1) structures have been shown.

Fig.3 (a) and (b) are schematics of the LEED patterns in Figs. 1b and 1c where o are diffraction spots from the Rh(111) surface, and ● are diffraction features from the oxygen overlayer. In (a) the reciprocal space unit cells of one domain of the c(2x2) and (2x1) structures are shown. In (b) the reciprocal space unit cell of a (2x2) structure is shown.

Fig.4 The basal plane of Rh_2O_3. The large circles represent oxide ions and the small circles represent Rh ions. The oxide ions are arranged in hcp lattice with a nearest neighbor distance of 2.949Å. The Rh ions occupy 2/3 of the octahedral holes with an in-plane nearest neighbor distance of 5.108Å. The unit cell of $Rh_2O_3(0001)$ is shown.[28]

Fig.5 AES spectra for clean (top), chemisorbed oxygen (middle), and epitaxial Rh_2O_3 (bottom) on the Rh(111) surface.

Fig.6 Low energy AES spectra for a Rh(111) surface with O_{515}/Rh_{302} peak-to-peak ratios of (a) 0.0, (b) 0.18, and (c) 0.25.

Fig.7 TDS spectra from chemisorbed oxygen on Rh(111).

Oxygen LEED Patterns on Rh(111)

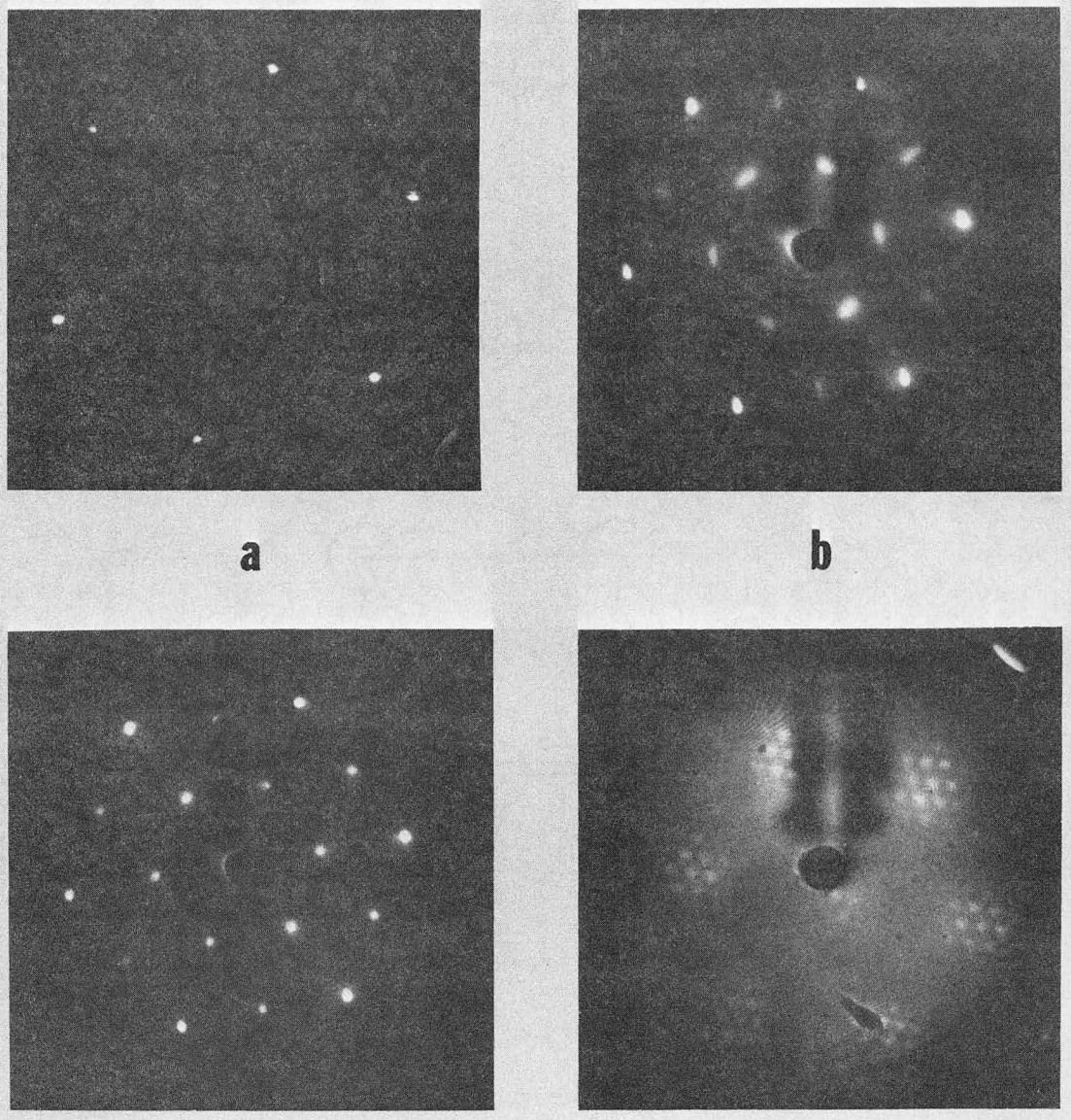

a b c d

XBB 788-10162

Fig.1

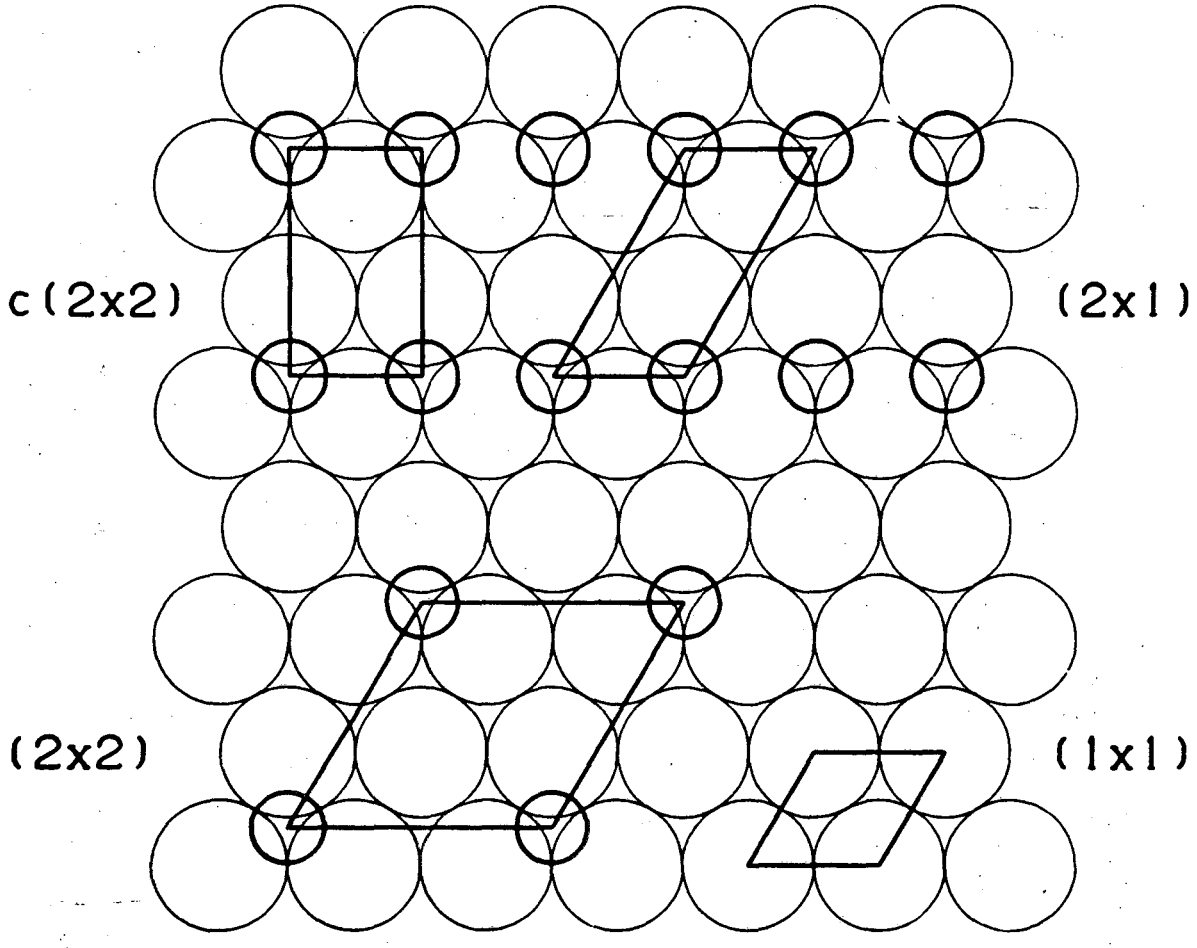

XBL 795-9676

Fig.2

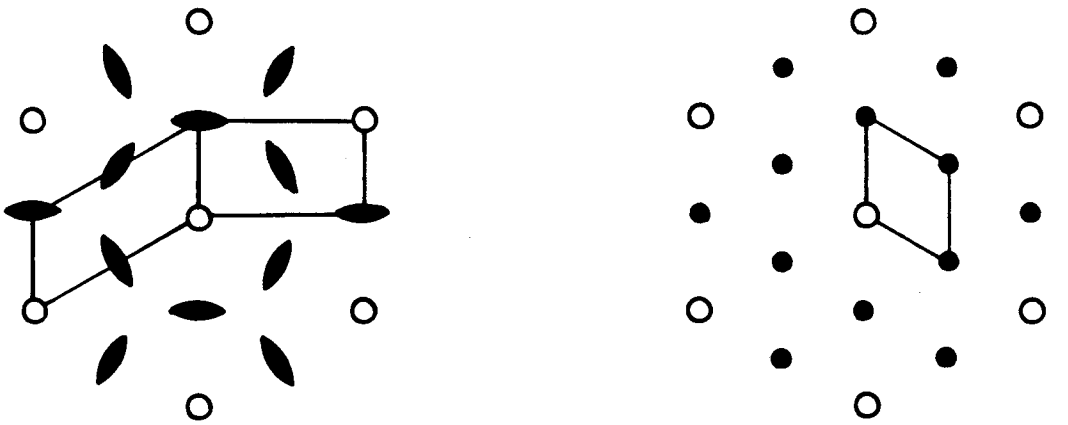

(a) (b)

XBL795-6308

Fig.3

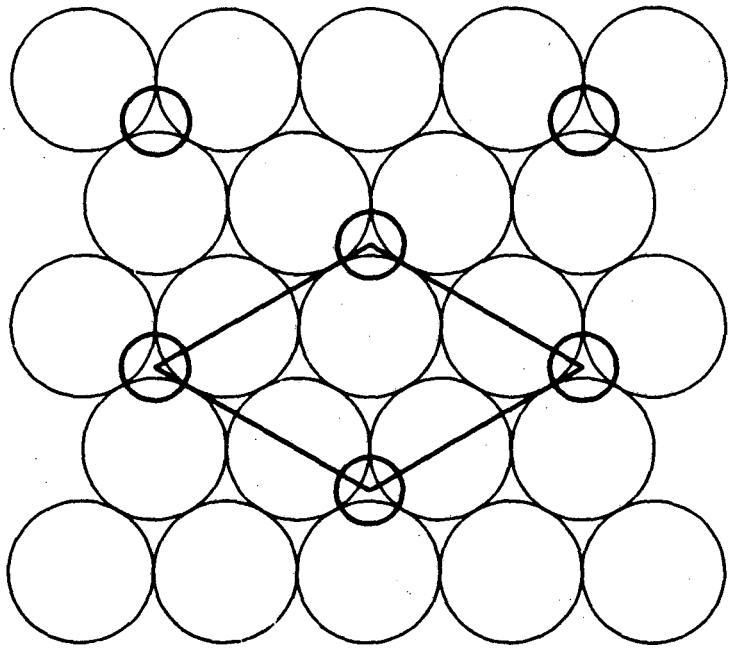

$Rh_2O_3(0001)$

XBL 795-9889

Fig.4

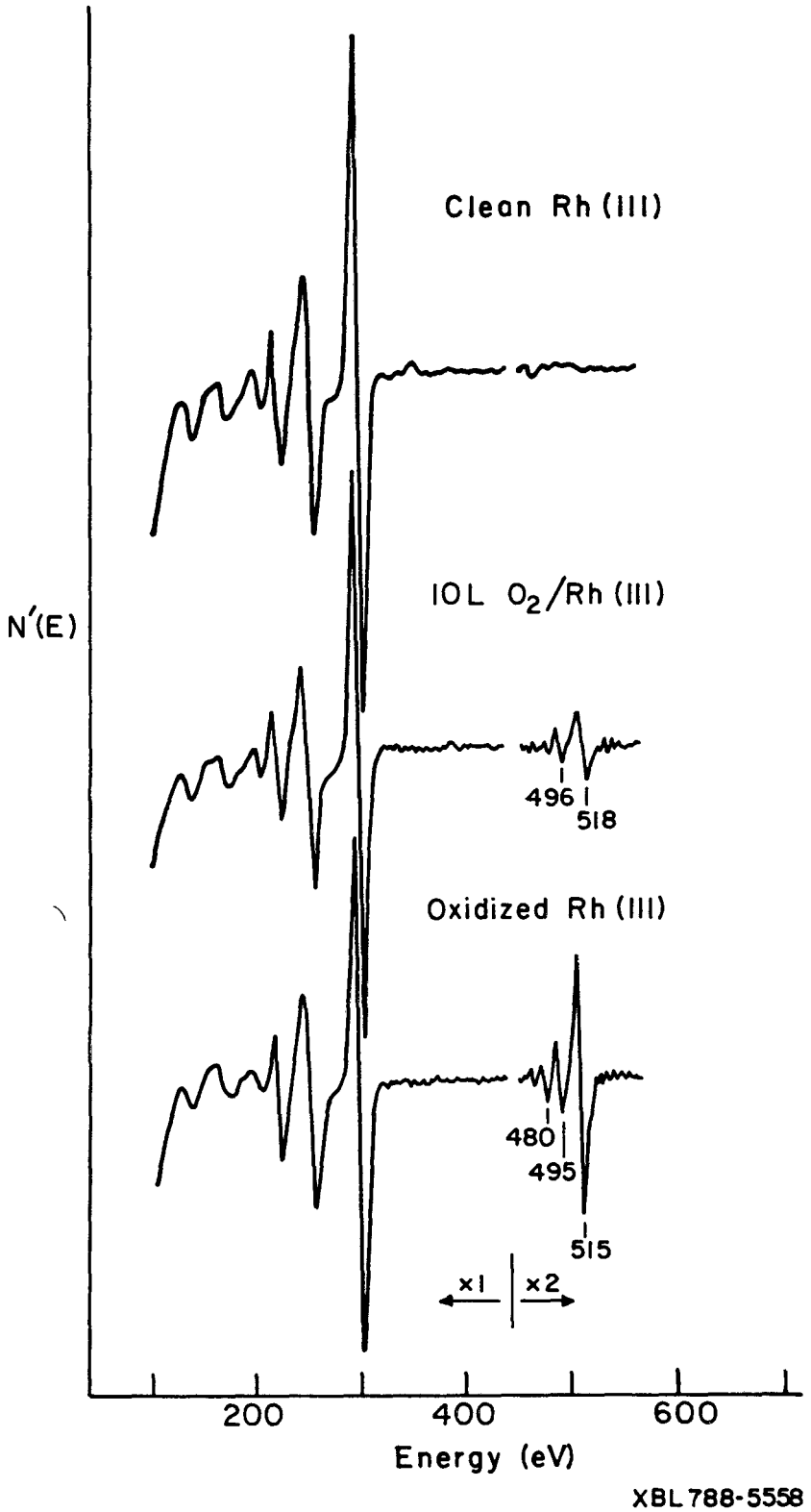
Clean Rh (III)
10L O_2/Rh (III)
N'(E)
496
518
Oxidized Rh (III)
480
495
515
x1
x2
200
400
600
Energy (eV)
XBL 788-5558

Fig.5

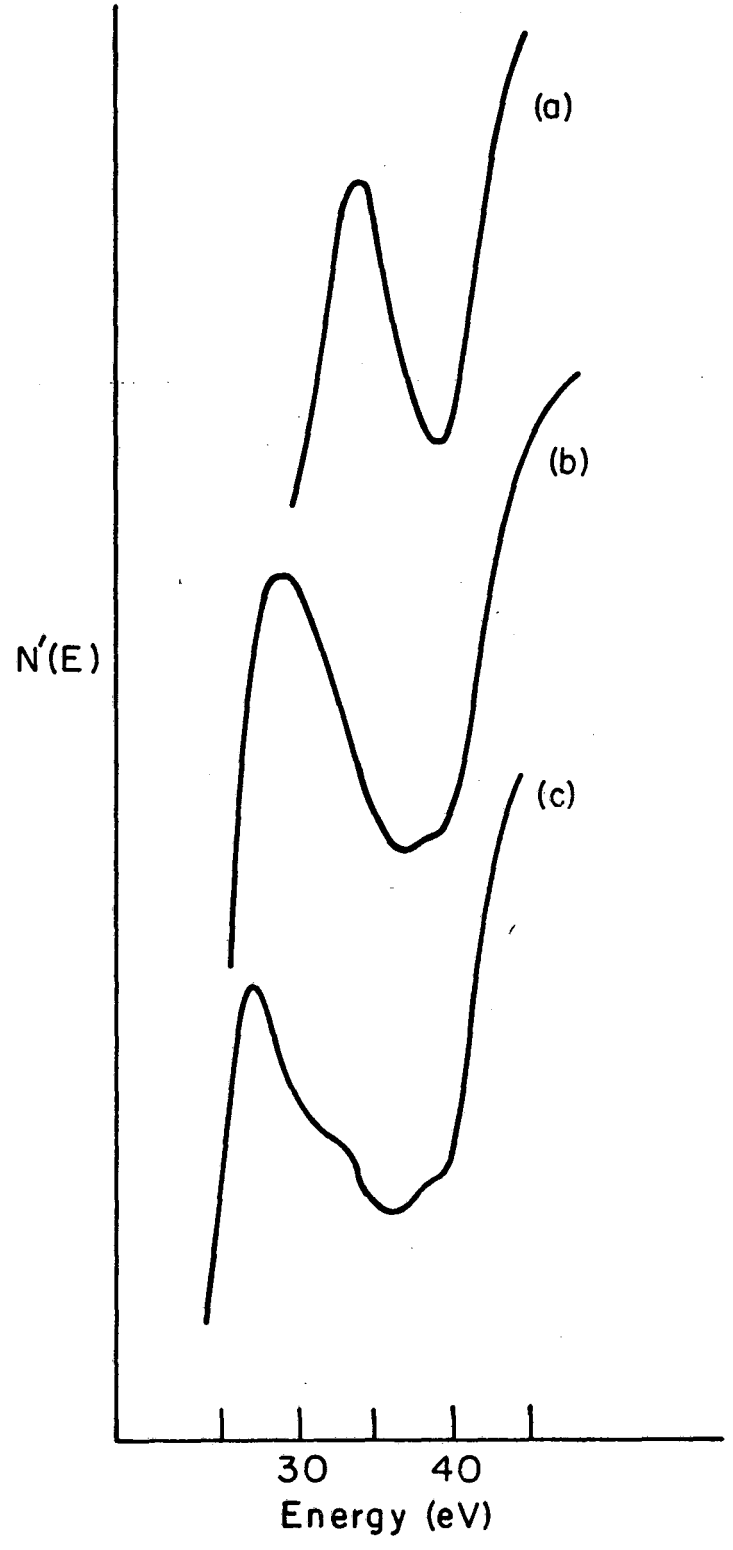

Fig.6

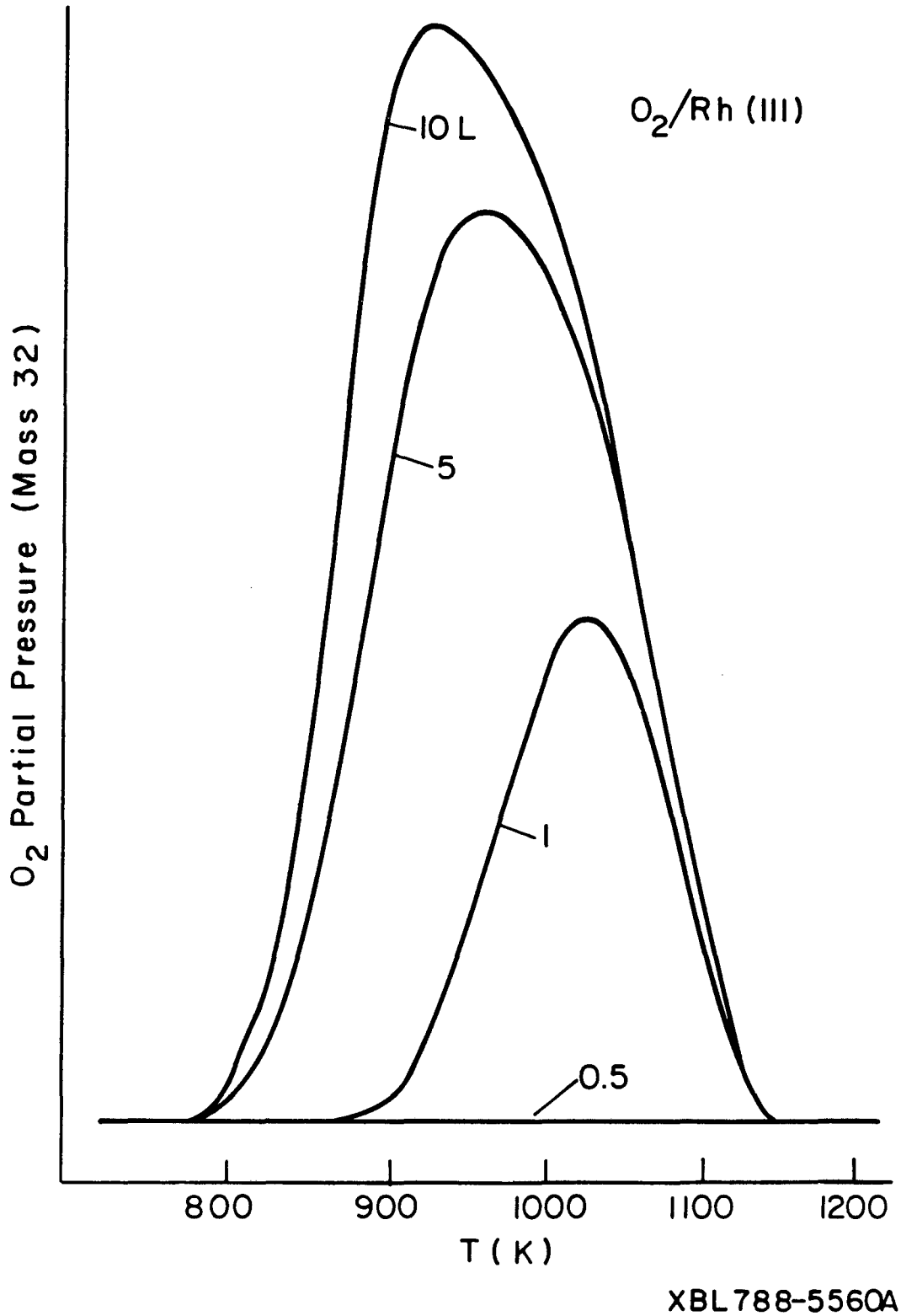
O_2/Rh (111)
10 L
5
1
0.5
O_2 Partial Pressure (Mass 32)
800
900
1000
1100
1200
T (K)
XBL788-5560A

Fig.7

This report was done with support from the Department of Energy. Any conclusions or opinions expressed in this report represent solely those of the author(s) and not necessarily those of The Regents of the University of California, the Lawrence Berkeley Laboratory or the Department of Energy.

Reference to a company or product name does not imply approval or recommendation of the product by the University of California or the U.S. Department of Energy to the exclusion of others that may be suitable.

TECHNICAL INFORMATION DEPARTMENT
LAWRENCE BERKELEY LABORATORY
UNIVERSITY OF CALIFORNIA
BERKELEY, CALIFORNIA 94720